WAVELET DE-NOISING AND GRADIENT ENHANCEMENT IN BIOMEDICAL IMAGE PROCESSING

Aleš Procházka and Eva Hošťálková
Department of Computing and Control Engineering
Institute of Chemical Technology in Prague
Technická 6, 166 28 Prague 6, Czech Republic
Email: A.Prochazka@ieee.org

Oldřich Vyšata
Neurocenter Caregroup
Jiráskova 1389, 516 01 Rychnov nad Kněžnou
Czech Republic
Email: vysata@neurol.cz

ABSTRACT
Detection of specific image components, their visualization and classification belong to main topics of biomedical image processing. The paper is devoted to problems related to the use of discrete wavelet transform (DWT) and the dual-tree complex wavelet transform (DTCWT) for image de-noising and to selected methods of its enhancement. The study presents the analysis of results achieved for different wavelet functions and the following application of gradient methods for specific image components detection. The information content of final images is followed both from the medical point of view using the previous experience and numerically through the analysis of image spectral components. The proposed methods indicate the efficiency of the dual-tree complex wavelet transform use in this area.

KEY WORDS
Image de-noising, discrete wavelet transform, gradient enhancement, biomedical image processing

1 INTRODUCTION

Image de-noising and analysis represent fundamental problems of image processing in various information systems. Problems closely related to this topic include signal restoration, enhancement [5], image segmentation [6, 17], recognition [1], classification, similarity detection [8] and noise analysis [2, 18]. Data acquisition forming the initial part of signal and image processing is followed by feature extraction, dimensionality reduction and compression in many cases as well.

The main part of the paper is devoted to wavelet transform use [3, 12, 15] and additive noise reduction by wavelet coefficients shrinkage. Both the discrete wavelet transform (DWT) and the dual-tree complex wavelet transform (DTCWT) are used for two-dimensional signal processing.

The proposed method is applied to various biomedical images of computed tomography (CT) and magnetic resonance (MR). An example of a set of MR images of the brain in the axial body plain is presented in Fig. 1. The paper is restricted to the two-dimensional signal processing enabling the extension of methods studied to the three-dimensional case.

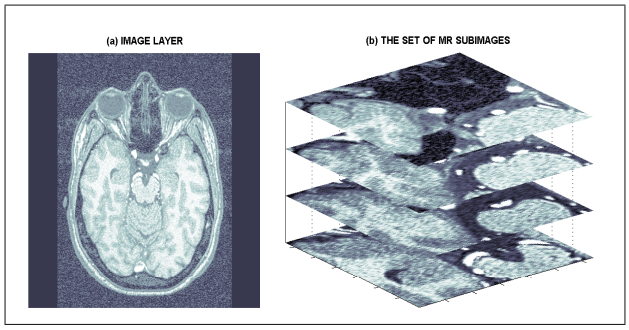

Figure 1. MR brain images presenting **(a)** an individual image and **(b)** layers selected from a set of MR images

2 WAVELET DECOMPOSITION AND RECONSTRUCTION

The DWT results in signal decomposition into a two-dimensional function of time and scale [7, 11] using the initial (mother) function $h(t)$. Its dilation and translation by coefficients a and b form the set of functions

$$h_{j,k}(t) = \frac{1}{\sqrt{a}}\, h(\frac{t-b}{a}) = \sqrt{2^j}\, h(2^j\, t - k) \qquad (1)$$

for integer values j, k in a diadic grid. Wavelet dilation corresponding to its spectrum compression enables the multi-resolution approach providing both global and local signal analysis using the Mallat decomposition tree [9]. Accordingly, a signal $x(t)$ for $t \in \langle 0, 1)$ can be decomposed into a superposition of shifted and dilated versions of the band-pass mother wavelet function [11] and the lowpass scaling function by relation

$$x(t) = c_0 + \sum_{j=0,1,\ldots} \sum_{k \in \mathcal{K}(j)} c_{2^j+k}\, h(2^j\, t - k) \qquad (2)$$

for $\mathcal{K}(j) = \{0, 1, \cdots, 2^j - 1\}$.

The DTCWT has been proposed [15] to overcome poor directional sensitivity of the DWT and to reduce shift sensitivity as well. The basic idea of this method is based upon the signal decomposition running in two parallel trees using real filters to generate real and imaginary parts of complex coefficients as outlined in Fig. 2.

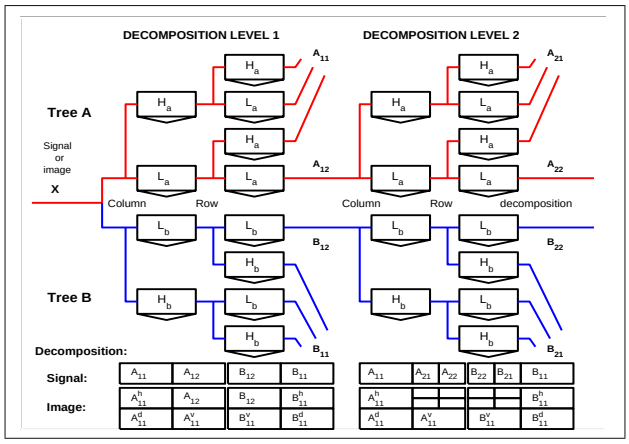

Figure 2. Principles of the dual-tree complex wavelet transform for signal or image analysis including downsampling by 2 in each decomposition level

In case of images, this process is carried out by firstly decomposing the image column-wise and then repeating the same procedure in the row direction. Eq. (2) can then be generalized [19] for decomposition of an image $X(t)$, $t \in \langle 0,1)\mathrm{x}\langle 0,1)$ as a superposition of shifted and dilated vertical, horizontal and diagonal two-dimensional wavelet functions and a lowpass two-dimensional scaling function for accordingly defined coefficients c_k.

An example of the analysis of the magnetic resonance image of the brain into the second level by the DWT and the DTCWT is presented in Fig. 3 and Fig. 4, respectively. In case of the DTCWT the number of the coefficients subbands is doubled as two decomposition trees are used improving thus directional selectivity of the wavelet coefficients at the expense of the moderate redundancy $2^2 : 1$ with respect to the DWT.

Wavelet-domain signals are used for multi-resolution signal or image analysis, compression and approximation [10, 19]. Some further tasks including signal de-noising can be used separately or as a preprocessing step of edge detection and possible extraction of features corresponding to the objects of interest and their subsequent classification.

The de-noising algorithm assumes an analyzed (multi-dimensional) signal to contain dominant low-frequency components and to be corrupted by additive noise with the power much lower than that of the analyzed signal. The whole method consists of the following steps:

1. Signal or image decomposition using a selected wavelet function up to a given level and evaluation of wavelet transform coefficients
2. Setting the threshold limits either individually for each coefficients subband at each level or globally for all wavelet coefficients
3. Thresholding the coefficients utilizing a chosen shrinkage method
4. Signal reconstruction from the modified wavelet coefficients and the original scaling coefficients

The result of this process highly depends on the choice of an appropriate wavelet function, a number of decomposition levels, threshold limits, and also a thresholding technique.

For soft thresholding, modification of the wavelet coefficients $\{c(k)\}_{k=0}^{N-1}$ by the threshold δ results in evaluation of new coefficients

$$\bar{c}_s(k) = \begin{cases} \text{sign } c(k)\ (|c(k)| - \delta) & \text{if } |c(k)| > \delta \\ 0 & \text{if } |c(k)| \leq \delta \end{cases} \tag{3}$$

The hard thresholding method results in the following values of coefficients

$$\bar{c}_h(k) = \begin{cases} \text{sign } c(k) & \text{if } |c(k)| > \delta \\ 0 & \text{if } |c(k)| \leq \delta \end{cases} \tag{4}$$

used for subsequent signal reconstruction.

These two wavelet shrinkage methods differ in the strategy of altering the coefficients greater than δ. Further techniques are based upon the use of specific thresholding functions. In this work, we choose soft thresholding assuming that large coefficients contain a similar amount of noise as the smaller ones.

The noise removal is used in this study as a preliminary step to edge detection. First of all, it is necessary to

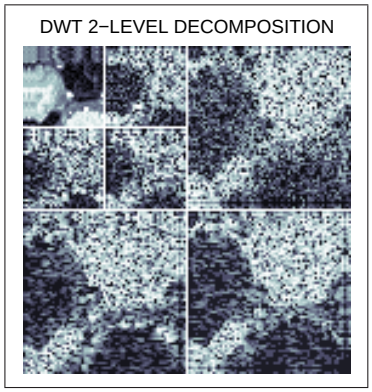

Figure 3. Decomposition of the MR brain image by the discrete wavelet transform into the second level using the Daubechies 8-tap filter

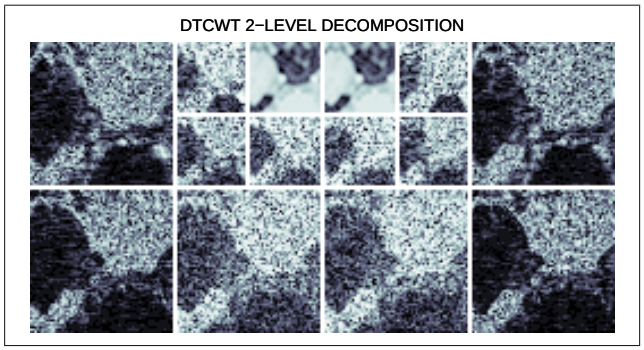

Figure 4. Decomposition of the MR brain image by the dual-tree complex wavelet transform into the second level with 16-tap q-shift filters [15]

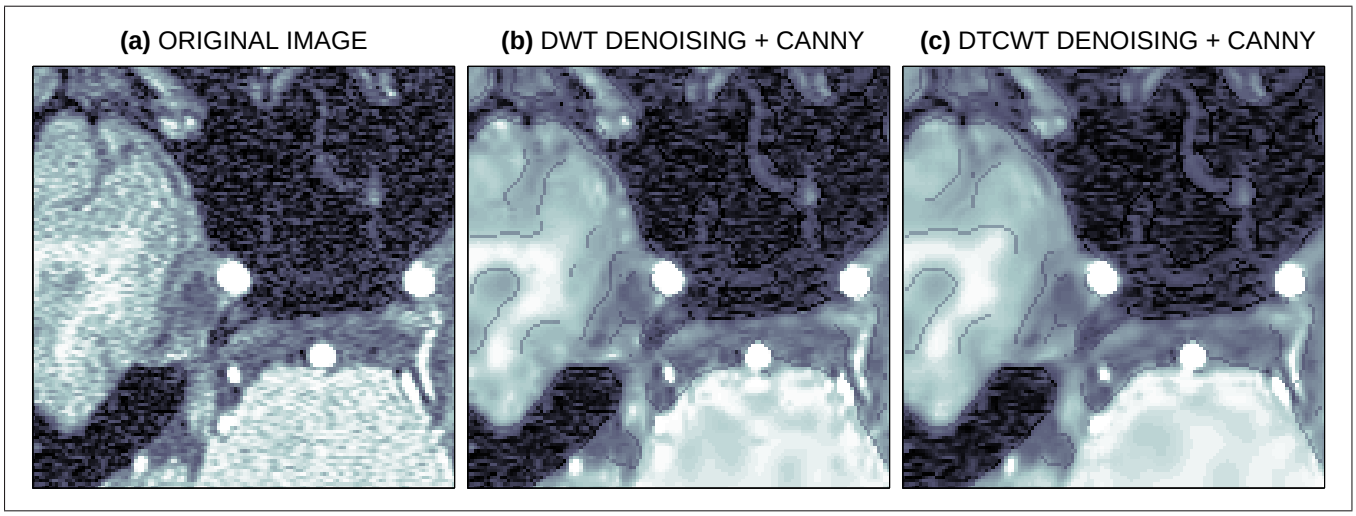

Figure 5. Axial MR brain image processing presenting **(a)** the original image, **(b)** and **(c)** images processed by the Canny edge detector after de-noising by wavelet shrinkage exploiting the DWT (14-tap symlet filters, 3 levels) and the DTCWT (14-tap q-shift filters, 3 levels)

estimate the noise standard deviation. For this purpose, the median absolute deviation (MAD) estimator is computed from the first level diagonal detail coefficients, which are supposed to be noise dominated

$$\hat{\sigma}_{mad} = \frac{median\{|c^d_{1,0}|, |c^d_{1,1}|, \ldots, |c^d_{1,N/4-1}|\}}{0.6745} \qquad (5)$$

where $c^d_{1,n}$ is the n-th diagonal detail coefficient of level 1 and N is the image size. The constant in the denominator applies to independent identically distributed Gaussian noise. The median approach is robust against large deviations of noise variance.

The estimated value of the standard deviation is used for calculation of the soft global threshold limit from the Donoho formula

$$\delta = \sqrt{2\ \hat{\sigma}^2_{mad}\ log(N)} \qquad (6)$$

The kind of wavelet filters and the number of decomposition levels is estimated due to the visual analysis of results.

3 EDGE DETECTION

Image edges can be looked upon as abrupt changes of the intensity represented by high frequencies in the Fourier domain. Sharp edges of a steep step-function profile may be easily detected by short gradient masks. The whole process is based upon the two-dimensional convolution [4, 13, 14] of a mostly odd-sized convolution kernel $\mathbf{H}_{K,J}$ and an image matrix $\mathbf{S}_{M,N}$ evaluating the elements of a new matrix $\mathbf{T}_{M,N}$ by relation

$$t_{m-\frac{K-1}{2},n-\frac{J-1}{2}} = \sum_{k=1}^{K}\sum_{j=1}^{J} h_{k,j}\ s_{m-k+1,n-j+1} \qquad (7)$$

for all values of m, n and selected boundary conditions. A new value is assigned to the pixel lying in the center of the odd-sized mask at each shift.

Methods of image wavelet de-noising can be efficiently combined with edge detection to reduce the effect of noise on gradient methods. This increases the robustness of the whole procedure as depicted in Fig. 8, where the compass (or Robinson) mask is used

$$\mathbf{H} = \begin{pmatrix} -1 & 1 & 1 \\ -1 & -2 & 1 \\ -1 & 1 & 1 \end{pmatrix} \qquad (8)$$

By rotation, this mask approximates the gradient in all eight possible directions. For every pixel, we chose the orientation with the highest convolution with the intensity of the neighbouring pixels.

These short-tap filters applied to blurred and noisy images either fail to detect an edge or tend to give false alarms. However, extending the tap length leads to blurring

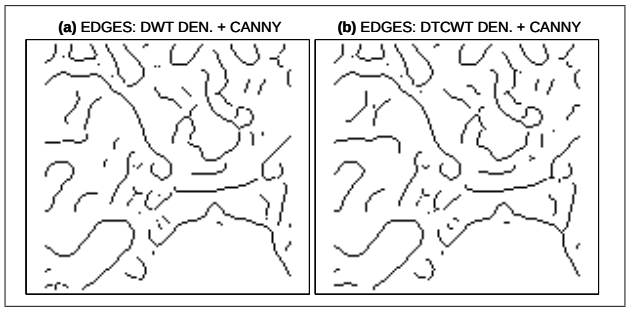

Figure 6. Edges detected by the Canny method (scale $\sigma = 1.8$) applied to the CT brain image after de-noising by wavelet shrinkage using **(a)** the DWT and **(b)** the DTCWT

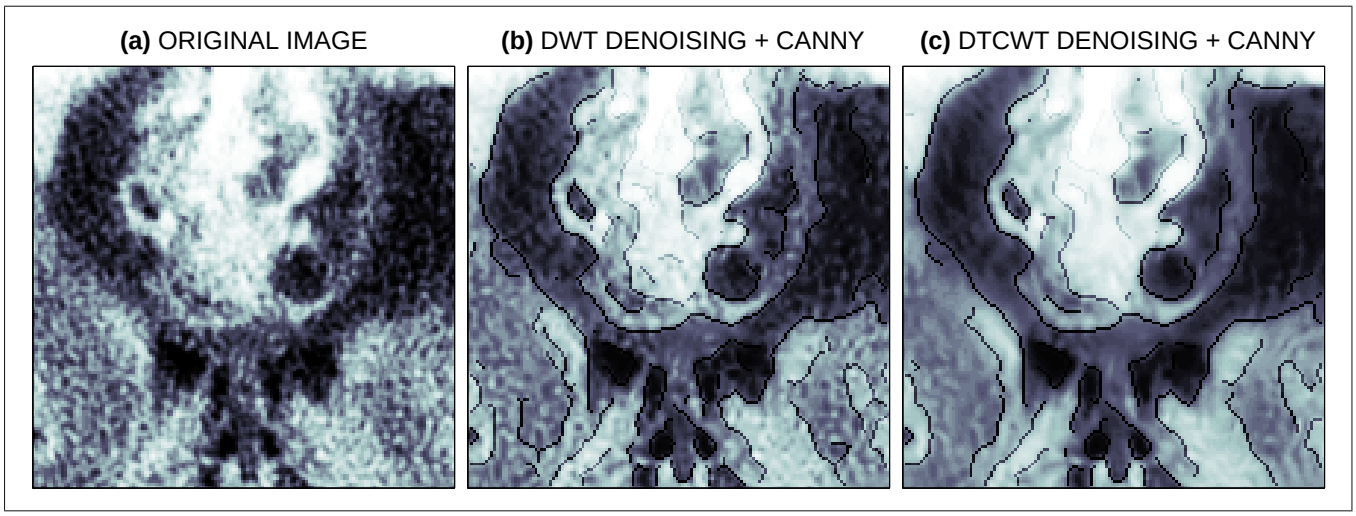

Figure 7. CT brain of a malignant tumor in the frontal lobes with tumor (white), necrosis (dark spots inside the tumor) and edema around the tumor (dark) presenting **(a)** the original image, **(b)** and **(c)** images processed by the Canny edge detector after de-noising by a shrinkage exploiting the DWT (16-tap symlet filters, 4 levels) and the DTCWT (16-tap q-shift filters, 4 levels)

the originally sharp edges. The problem lies in attempting to detect edges of different spatial sizes by a single-scale filter. It is more convenient to analyze images by multi-scale methods, such as the Canny detector.

The Canny filter approximates the first derivative of a two-dimensional (2D) Gaussian in the direction of the gradient. This method is robust against noise because of using a Gaussian filter to smooth the data prior to edge detection and providing a selective algorithm for identifying weak edges.

A 2D Gaussian low-pass filter is separable. Hence we may subsequently convolve the image with two 1D Gaussian masks in the row and the column directions. For σ denoting the standard deviation and the 2D Gaussian

$$G(x,y) = C\, e^{-\frac{(x^2+y^2)}{2\sigma^2}} \tag{9}$$

it is possible to apply the convolution of its derivative in both directions with the given image. These two results are combined together into a matrix whose elements are thresholded to identify pixels corresponding to strong edges. The rest of the pixels may be assigned to weak edges only if their values are greater than the lower threshold limit and if their gradient corresponds to the direction of the stronger edges in the neighborhood. The extracted edges after erosion are shown in Fig. 6.

As the next step, the edge images are combined with the de-noised images. Fig. 5 and Fig. 7 depict the Canny method applied to selected de-noised CT and MR biomedical images of the brain.

By adjusting the value of standard deviation σ, the Canny detector may operate at various scales. For the MR image in Fig. 5 we selected $\sigma = 2.5$ and for the CT image in Fig. 7 the values $\sigma = 1.8$ has been used.

4 RESULTS

The wavelet image de-noising using both the DWT and the DTCWT for different wavelet functions has been applied to selected biomedical images with the following gradient image enhancement. The main purpose of this process is in the detection of specific biomedical image components in their early stages and their visual enhancement.

To analyse the results it is possible to study the two-dimensional discrete Fourier transform of the original and enhanced images and their spectral components. Fig. 9(a) presents the contour plot of the spectrum belonging to the original biomedical image of the brain. The de-noising procedure applied to reduce the image noise should reject high-frequency components and to preserve low-frequency parts including their frequency multiples responsible for abrupt image changes.

Fig. 9(b) and (c) present contour plots of image spectra after the use of the DWT (using db4 wavelet) and DTCWT. It is obvious that high-frequency components are more substantially rejected by the DTCWT even though the balance must be achieved between this process and preservation of low-frequency components and image edges.

Statistical comparison of different wavelet functions use for processing of selected biomedical images is presented in Table 1. Numerical results include the mean and the standard deviation of high-frequency image components estimated by the two-dimensional discrete Fourier transform and selection of frequency components in the upper half of the frequency ranges in both image directions. Results presented in Table 1 and the corresponding Fig. 10 show that the DTCWT decreases image energy in this frequency range in comparison with the DWT. Results obtained have been verified by the neurologist specialised in the analysis of biomedical images as this process is very

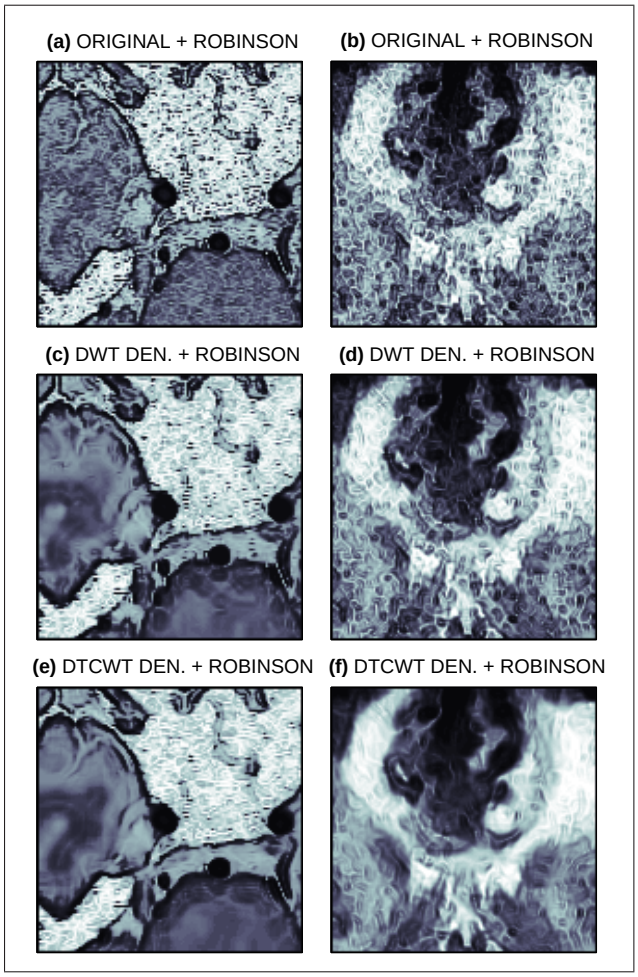

Figure 8. Convolution of the Robinson filter with **(a)**, **(b)** the original MR and CT brain images, resp., **(c)**, **(d)** the images after DWT de-noising, and **(e)**, **(f)** the images after the DTCWT de-noising

sensitive and no important image features must be rejected. Results achieved point to the efficiency of the dual-tree complex wavelet transform.

In addition to the process of spectral analysis of de-noised images differences between original and de-noised images have been studied as well to find statistical properties of the image noise.

5 CONCLUSIONS

The paper is devoted to the use of the wavelet transform for noise removal and enhancement of biomedical images. Both the discrete wavelet transform and the dual-tree complex wavelet transform are studied along with gradient edge detection. The paper provides also the study of the compass gradient mask and the Canny edge detector use for biomedical images. Both the numerical results and expert opinion provide promising support for the future work in this field.

Problems of image de-noising and enhancement are closely related with many other research topics including

Table 1. ANALYSIS OF SPECTRAL COMPONENTS IN THE UPPER HALF OF THE FREQUENCY RANGES OF BIOMEDICAL IMAGES DE-NOISED BY THE DWT AND DTCWT

Data	*Wavelet*	*De-Noised Image*			
		Mean		*STD*	
		DWT	DTCWT	DWT	DTCWT
Brain (CT)	db4	1.61	0.46	1.02	0.32
	db8	1.57		0.99	
	haar	1.42		0.82	
	sym3	1.61		0.97	
Brain (MR)	db4	0.002	0.0007	0.002	0.0004
	db8	0.001		0.001	
	haar	0.003		0.002	
	sym3	0.002		0.002	
Back-bone	db4	6.94	6.51	3.81	3.56
	db8	6.71		3.67	
	haar	7.15		3.96	
	sym3	6.98		3.82	
Kidney	db4	0.75	0.45	0.44	0.26
	db8	0.58		0.35	
	haar	0.85		0.49	
	sym3	0.76		0.44	

adaptive methods of image de-noising [16] and the appropriate image resolution choice. The future work will be devoted to these problems as well covering also the spline interpolation generalized to three-dimensions to increase the resolution of MR layers sets.

Interpolation methods and image modelling methods will be further studied as important tools for reconstruction of image components spoiled by various artifacts, along with the three-dimensional wavelet image de-noising and enhancement to detect specific image components.

Accompanying tasks will include the evolution of appropriate visualization methods and application of distributed computing tools to enable fast enough multi-dimensional and multi-scale signal processing.

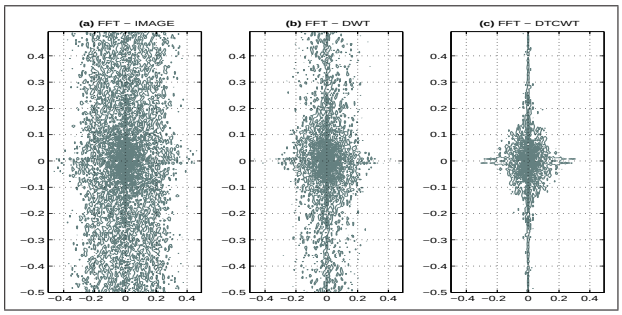

Figure 9. Spectral components of the **(a)** original image of the brain, **(b)** de-noised image using the db4 wavelet, and **(c)** de-noised image after the dual-tree complex wavelet transform use

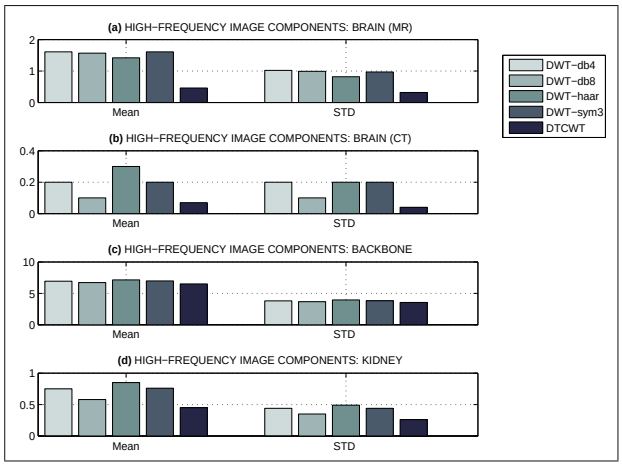

Figure 10. Comparison of high-frequency spectral components features for different biomedical images and different de-noising methods

6 ACKNOWLEDGMENTS

The paper has been supported by Research grant No. MSM 6046137306. Real data sets have been collected by the Neurocenter Caregroup in Rychnov nad Kneznou. The dual-tree complex wavelet transform library has been kindly provided by prof. N. Kingsbury [7] from the Engineering Department of the University of Cambridge, U.K.

References

[1] R. Anderson, N. Kingsbury, and J. Fauqueur. Rotation-Invariant Object Recognition Using Edge Profile Clusters. In *The European Signal Processing Conference EUSIPCO-06*. EURASIP, 2006.

[2] C. Chaux, J. C. Pesquet, and L. Duval. Noise Covariance Properties in Dual-Tree Wavelet Decomposition. *IEEE Transaction on Information Theory*, 53(12):4690–4700, December 2007.

[3] J. Fauqueur, N. Kingsbury, and R. Anderson. Multiscale Keypoint Detection Using the Dual-Tree Complex Wavelet Transform. In *The ICIP-06 Conference*. IEEE, 2006.

[4] R. C. Gonzales, R. E. Woods, and S. L. Eddins. *Digital Image Processing Using MATLAB*. Prentice Hall, 2004.

[5] J. H. Jang, Y. S. Kim, and J. B. Ra. Image Enhancement in Multi-Resolution Multi-Sensor Fusion. In *The IEEE Conference on Advanced Video and Signal Based Surveillance*, pages 289–294. IEEE, 2007.

[6] F. S. Jones. Medical Image Segmentation. Master's thesis, University of Georgia, Athens, 2003.

[7] N. G. Kingsbury. Complex Wavelets for Shift Invariant Analysis and Filtering of Signals. *Journal of Applied and Computational Harmonic Analysis*, 10(3):234–253, May 2001.

[8] M. Lee, L. Liu, and M. Chen. Similarity Analysis of Time Series Gene Expression Using Dual-Tree Wavelet Transform. In *The 32nd International Conference on Acoustics, Speech and Signal Processing*, pages I–413–I–416. IEEE, 2007.

[9] S. Mallat. A theory for multiresolution signal decomposition: The wavelet representation. *IEEE Trans. Pattern Anal. Mach. Intell.*, 11(7):674–693, 1989.

[10] S. Mallat. *A Wavelet Tour of Signal Processing*. Accademic Press, San Diego, 1999.

[11] D. E. Newland. *An Introduction to Random Vibrations, Spectral and Wavelet Analysis*. Longman Scientific & Technical, Essex, U.K., third edition, 1994.

[12] N.G. Kingsbury and J.F.A. Mugarey. Wavelet Transforms in Image Processing. In A. Procházka, J. Uhlíř, P. J. W. Rayner, and N. G. Kingsbury, editors, *Signal Analysis and Prediction*, Applied and Numerical Harmonic Analysis, chapter 2. Birkhauser, Boston, U.S.A., 1998.

[13] Rae-Hong Park. Complex-Valued Feature Masks by directional Filtering of 3 x 3 Compass Feature Masks. *Pattern Recognition and Applications*, 5:363–378, 2002.

[14] M. Petrou and P. Bosdogianni. *Image Processing*. John Wiley & Sons, 2000.

[15] I. W. Selesnick, R. G. Baraniuk, and N. G. Kingsbury. The Dual Tree Complex Wavelet Transform. *IEEE Signal Processing Magazine*, 22(6):123–151, November 2005.

[16] M. Srinivasan and S. Annadurai. Adaptive Multiscale Image Denoising Using Neural Networks. In *The 2004 International Conference on Signal Processing and Communications SPCOM*. IEEE, 2004.

[17] B. Sumengen and B. S. Manjunath. Multi-Scale Edge Detection and Image Segmentation. In *The European Signal Processing Conference EUSIPCO-05*. EURASIP, 2005.

[18] S. V. Vaseghi. *Advanced Digital Signal Processing and Noise Reduction*. John Wiley & Sons Ltd, West Sussex, 2006.

[19] M. B. Wakin, J. K. Romberg, H. Choi, and G. Baraniuk. Wavelet-Domain Approximation and Compression of Piecewise Smooth Images. *IEEE Transactions on Image Processing*, 15(6):1071–1087, 2006.